Mission Research Corporation

Copy No. 3

MRC-R-1375

EMP ON A NTS EXPERIMENT

Jim Gilbert
Victor van Lint
Steve Sherwood

October 15, 1991

Subcontract No. 9-XS8-7967R-1

Prepared by: MISSION RESEARCH CORPORATION
735 State Street, P.O. Drawer 719
Santa Barbara, California 93102

SECTION I
INTRODUCTION

This report is a compilation of two previous sets of pretest calculations, references 1 and 2 and the grounding and shielding report, reference 3. The calculations performed in reference 1 were made for the baseline system, with the instrumentation trailers not isolated from ground, and wider ranges of ground conductivity were considered. This was used to develop the grounding and shielding plan included in the appendix. The final pretest calculations of reference 2 were performed for the modified system with isolated trailers, and with a better knowledge of the ground conductivity.

The basic driving mechanism for currents in the model is the motion of Compton electrons, driven by gamma rays, in the air gaps and soil. Most of the Compton current is balanced by conduction current which returns directly along the path of the Compton electron, but a small fraction will return by circuitous paths involving current flow on conductors, including the uphole cables.

The calculation of the currents is done in a two step process - first the voltages in the ground near the conducting metallic structures is calculated without considering the presence of the structures. These are then used as open circuit drivers for an electrical model of the conductors which is obtained from loop integrals of Maxwell's equations. The model which is used is a transmission line model, similar to those which have been used to calculate EMP currents on buried and overhead cables in other situations, including previous underground tests, although on much shorter distance and time scales, and with more controlled geometries. The behavior of air gaps between the conducting structure and the walls of the drift is calculated using an air chemistry model which determines the electron and ion densities and uses them to calculate the air conductivity across the gap.

Section II of this report discusses the EMP driver terms, and basic physical parameters of the air and soil models. Section III discusses the basis of the transmission line electrical model, including the special models which had to be developed to account for the air gaps, rockbolts and isolated trailers. In section IV, the calculational results are presented, including both the scoping calculations of reference 1 and the pretest calculations of reference 2. In this section, the pretest predictions are also compared with the experimental data.

SECTION II
EMP DRIVER TERMS

Compton Currents

The dominant driver for EMP fields out to hundreds of microseconds after zero time is the displacement of electrons in the air voids and soil by gamma rays. The gamma rays include both prompt gammas and those produced by neutron capture and inelastic reactions. If the flux of monoenergetic gamma rays of energy E_γ MeV is f_γ MeV per square meter per second, the Compton current in amperes per square meter per second is

$$J_c = \frac{e \lambda_e f_\gamma}{\lambda_\gamma E_\gamma}$$

where e is the electronic charge, λ_e is the mean forward range of the of the electron ejected by the Compton effect, and λ_γ is the range of the gamma, which, at the few MeV energies typical of EMP problems, interacts with materials almost entirely through the Compton effect.

Two features of this process lead to considerable simplification in calculating EMP source currents. The first is that the ratio of the Compton current to the gamma flux is only weakly dependent on the energy of the gamma rays as the range of the Compton electron increases a little more rapidly than the energy, and the range of the gamma rays increases only slightly with energy. For gamma ray energies between 1 and 5 MeV, the current to flux ratio varies only 6% from the average value (reference 4), so that we can use the average value without introducing much error. The second feature which leads to simplification is that the mean forward range (measured in grams/cm^2) of the Compton electrons is only weakly dependent on the material - The mean forward range in air of a 1 MeV electron is only about 10% longer than it is in aluminum or silicon, and we ignore these variations as well. Very large atomic number materials have much shorter forward ranges due to scattering in the nuclear fields - under the same conditions, the mean forward range in lead is only about half that of aluminum. As noted before, the Compton cross section is weakly dependent on energy, and, when measured in square centimeters per gram, is independent of material for typical materials with one electron per two atomic mass units. This means that the Compton current can be taken to be proportional to the gamma dose rate for situations where the gamma flux is directed (when the gamma flux is isotropic, the Compton currents will, of course, cancel). If the gamma dose rate in rads per second is D-dot, the Compton current in amperes per square meter is

$$J_c = 2\times10^{-8}\,\dot{D}$$

The absorption length of the gammas is somewhat dependent on their energy, ranging from 37 gm/cm^2 for 1 MeV gammas to 58 gm/cm^2 for 6 MeV gammas (reference 3). For this study we will use 40 gm/cm^2 which is characteristic of 1.5 MeV prompt gammas and a soil density of 2 gm/cm^3.

Air Conductivity

A second quantity of interest in calculating the EMP drivers is the conductivity of the medium. In this calculation, we are interested in two media - the first is air in the tunnels and the second is compacted alluvium. The radiation induced conductivity of air is dependent on the number of free electrons and ions. The rate of production of free electrons by Compton electrons is proportional to the dose rate with one electron being produced per 34 eV of energy, or about 30,000 per Compton electron. The dominant mechanism reducing the density of free electrons is three body attachment to O_2, forming the O_2^- ion. This attachment typically occurs in about ten nanoseconds. Water is very effective as a third body in the reaction, and the rate of this reaction is very sensitive to water content in the range of a few percent by molecular concentration. The attachment rate also depends strongly on the energy of the free electrons. The numeric code used for the calculations tracks the electron densities by numerically integrating the equations for the electron and negative ion densities

$$\frac{\partial N_e}{\partial t} = S_i - \alpha_e(E)\, N_e$$

$$\frac{\partial N_-}{\partial t} = \alpha_e(E)\, N_e - \beta\, N_-\, N_+$$

$$\frac{\partial N_+}{\partial t} = S_i - \beta\, N_-\, N_+$$

where α_e(E) is the rate of attachment of electrons, S_i is the ionization rate and β is the rate of recombination of ions. Dependence on the electric field E of the attachment rate is shown explicitly. The conductivity is then given by

$$\sigma = e\, \mu_e(E)\, N_e + e\, \mu_i(N_+ + N_-)$$

where μ_e and μ_i are the electronic and ionic mobilities, respectively. As the ionic mobility is much less than the electronic mobility, the ions are only dominant at low dose rates when their density is much greater than that of the electrons. For moist air, the conductivity is approximately given by

$$\sigma = 3\times10^{-13}\, \dot{D} + 2.5\times10^{-9}\sqrt{\dot{D}}$$

where the first term is from the electrons and the second term is from the ions.

Soil Conductivity

As will be seen in the numerical calculations, the results are sensitive to the assumed soil conductivity. For the range of radiation levels encountered in this experiment, the enhancement of soil conductivity is expected to be small. A measurement between wellheads has indicated a conductivity of about 10^{-2} mho/m. The resistance between two parallel cylinders each of length l and radius s, separated by a distance s is

$$R = \frac{\ln(l/r)}{\pi\sigma l} - \frac{1}{\pi s\sigma} = 2.4 \quad ohms$$

where σ is the ground conductivity in mho/m, as long as the separation is somewhat longer than their length and the length is much shorter than a skin depth, or

$$l < \sqrt{\frac{1}{\mu_0 \sigma \omega}}$$

When this is solved for the conductivity, we obtain

$$\sigma = 1.2\times10^{-2} \quad ohms$$

The conductivity from wave tilt measurements at about one megahertz indicate that, throughout much of the basin and range area, the ground conductivity is on the order of 4×10^{-3} mho/m as can be noted from figure 1 taken from reference 6. Some other relevant conductivities from reference 2 are 3×10^{-2} mho/m for Yucca Flat ground water and 10^{-3} mho/m for alluvium. The set of calculations in reference 1 included soil conductivities as low as 2×10^{-3}, but as both the well logging and the wellhead measurements indicate conductivities on the order of 10^{-2}, we have used this and a factor of two excursion above and below this value for the baseline calculations.

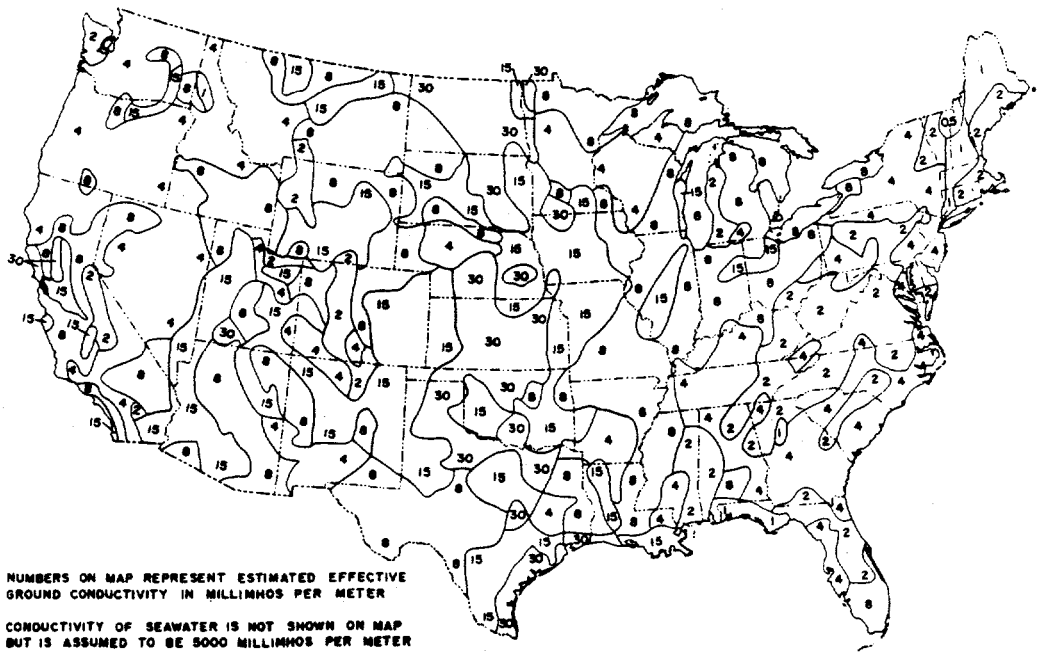

Figure 1 Ground conductivity in US from 1 MHz wave tile measurements (from reference 6)

SECTION III
ELECTRICAL MODEL

A Simple Case

A simple illustrative case is a conducting sphere in the ground which constantly emits gammas symmetrically in a radial direction. We assume that the radius of the sphere is several meters, so that the absorption of gammas in the ground is much larger than their $1/r^2$ divergence. The sphere rises to a positive voltage with respect to distant ground. The radial electric field obeys the equation

$$\epsilon_0 \frac{\partial E_r}{\partial t} + \sigma E_r + J_c = 0$$

The first term vanishes in steady state, so that the voltage, which is the radial integral of the electric field is given by (for sigma$=1.5 \times 10^{-2}$ mho/m)

$$V = \frac{1}{\sigma} \int J_c \, dr \approx \frac{J_c \lambda_\gamma}{\sigma} \approx 2.7 \times 10^{-7} \dot{D}$$

Now let us take this case and modify it slightly by placing a second sphere,which does not emit gammas, many radii away, and connecting the two spheres with an insulating cable. If the radius of each sphere is r_0, the resistance of each sphere to distant ground is

$$R = \frac{1}{4\pi\sigma r_0}$$

and the current that will flow on the insulating cable is

$$I = \frac{V}{2R}$$

The fraction of the total Compton current leaving the sphere that flows on the insulating cable is independent of the soil conductivity and is

$$\frac{I}{4\pi r_0^2 J_c} = \frac{\lambda_\gamma}{2r_0}$$

which is small under our assumption that the λ_γ was small compared to the sphere's radius. When we start to model time dependent phenomena, the situation becomes a little more complicated, and we will first digress to a study of the modelling of long thin structures by using the telegrapher's equations, also known as the transmission line technique.

Transmission Line Equations

The technique which is used to model long thin structures is based on performing loop integrals of Maxwell's equations. For a moment, let us consider cases which have cylindrical symmetry, but have variations along the axial direction which we will denote as z. Figure 2 shows a simple case with a conducting cylinder surrounded by a layer with a conductivity which can be different from the surrounding soil. The first of the telegrapher's equations in a medium without sources is derived by integrating

$$\nabla \times E = -\mu \frac{\partial H}{\partial t}$$

around the loop shown. Define the impedance Z by

$$Z I(z,t) = \mu \frac{\partial}{\partial t} \int_a^\infty dr\ H_\phi$$

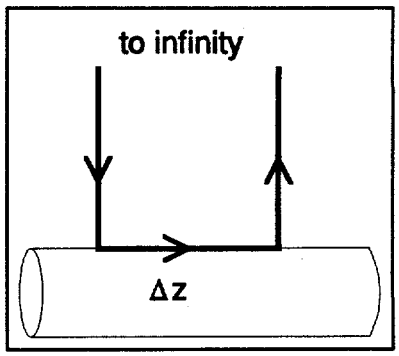

Figure 2 Integration path for first transmission line equation

and

$$V = \int_a^\infty dr\ E_r$$

where Z is an, as yet undefined, linear operator in z and t. Taking the limit as $\Delta z \to 0$ we obtain

$$Z I + \frac{\partial V}{\partial z} = 0$$

The second of the telegrapher's equations is derived by integrating

$$\nabla \times H = \epsilon \frac{\partial E}{\partial t} + \sigma E$$

over the path shown in figure 3. With the definitions

$$I(z,t) = 2\pi a\, H_\phi(r=a)$$

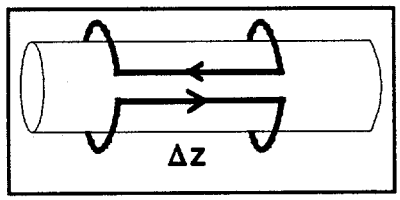

Figure 3 Integration path for second transmission line equation

and

$$YV = 2\pi a \left(\epsilon_0 \frac{\partial}{\partial t} + \sigma\right) E_r(r=a)$$

we obtain the second of the telegrapher's equations

$$YV + \frac{\partial I}{\partial z} = 0$$

Now we haven't really said anything yet - we have just put all of the physics into two unknown linear operators in z and t which we have denoted as Z and Y. These operators depend on the radial dependence of the magnetic and electric fields, which we don't know. We will make approximations to these quantities. The first approximation is that we will assume that the parameters are independent of location on z. This is rigorously true for TEM modes on transmission lines, but is also satisfied for many other situations when the skin depth in the medium surrounding the conductors is much longer than the radius of the conductors. The second approximation is that either the conductivity or the dielectric constant dominates the radial solutions which determine Y. When the system is in contact with the soil, the conduction term dominates for frequencies of interest and Y is a conductance per unit length. When part of the system is insulated, such as the uphole cables below the wellheads, the term proportional to the dielectric constant dominates and Y is the capacitive admittance per unit length. The third approximation is that Z contains a inductive part and a resistive part. With these approximations, which have been often compared with analytic and multidimensional numerical results, the telegraphers equations become

$$L\frac{\partial I}{\partial t} + RI + \frac{\partial V}{\partial z} = 0$$

and, for portions of the system in contact with the soil,

$$GV + \frac{\partial I}{\partial z} = 0$$

For portions of the system insulated from the soil

$$C\frac{\partial V}{\partial t} + \frac{\partial I}{\partial z} = 0$$

The finite difference form of the above equations result in a matrix which is tridiagonal and can be inverted by using an LU decomposition. This is extremely rapid and permits the use of time steps which follow physical variation of the voltage and current rather than being forced to be small by a condition analogous to the Courant condition of hydrodynamics.

Line Parameters

The inductance per unit length is determined by the distance into the ground which the magnetic fields extend. From reference 7, we obtain currents close to those from an analytic solution if we assume that the magnetic fields and electric fields behave as 1/r out to a skin depth, and are zero outside that radius. This gives us an approximation for the inductance

$$L = \frac{\mu_0}{2\pi}\ln(\delta/r)$$

where r is the radius of the conductor and the skin depth δ is

$$\delta = \sqrt{\frac{2t}{\mu_o \sigma}} \leq 300 \ meters$$

Note that the skin depth has been cut off at the length of the longest conductor. This is so that the late time current is in agreement with the static solution on a line of finite length. The conductance is given by

$$G = \frac{2\pi\sigma}{\ln(\delta/r)}$$

The series resistance per unit length is also obtained by comparison with solutions in the frequency domain.

$$R_{series} = \frac{1}{\pi\sigma\delta^2}$$

The driver is the shunt current per unit length which would produce the open circuit voltage of equation 12 in the absence of currents on the structure. This is

$$I_{driver} = \frac{J_c \lambda_\gamma}{\sigma} G$$

and the second transmission line equation becomes

$$GV + \frac{\partial I}{\partial z} = I_{driver}$$

Air Gaps and Rockbolts

We need to modify these equations to account for a couple of features in the geometry. The first of these is the modification of the driver when there is an air gap present around the tunnel. Then the driver becomes the sum of two terms, one for currents in the gap and a second for the currents in the soil on the far side of the gap. As the attenuation of gamma rays in the gap is negligible, it is fairly easy to see that, for a gap of width d,

$$I_{driver} = J_c G \left(\frac{d}{\sigma_a} + \frac{\lambda_\gamma}{\sigma_g} \right)$$

where the subscripts indicate the conductivity in the air or ground. There is an additional modification which is due to the rock bolts - the wire mesh is held to the wall by a series of rockbolts with a length of two meters and a spacing of 2 meters. The effect of the rockbolts is to increase the effective air conductivity by providing an additional shunt path for the return of the Compton current. Since the skin depth is longer than these rods for times of interest, we can use a static solution to the transmission line

equations to determine the effect of the rods. With most of the voltage appearing across the air gap and the first 10 cm of the soil, the bulk of the volume around the rockbolts is held at a voltage V with respect to the mesh (and the rockbolts). From the transmission line equation

$$GV + \frac{\partial I}{\partial z} = 0$$

so the current on the rockbolt is

$$I_{bolt} = G\,l\,V = \frac{2\pi l \sigma_g}{\ln(s/a)}$$

where l is the length of the rockbolt, s is the spacing and a is the radius. The current across the air gap is

$$I_{air} = \frac{s^2 \sigma_a V}{d}$$

so that the effect is to modify the air conductivity σ_a to an effective conductivity of

$$\sigma_a + \frac{2\pi\, d\, l\, \sigma_g}{s^2 \ln(s/a)}$$

Another feature is presence of the gap in the system of conductors between the instrumentation alcoves and the main pipe. This was modelled as a lumped resistance in one cell with a value of

$$R_{gap} = \frac{1}{2\pi r \sigma}$$

In the cases with an air gap, the gap only went partially around the system. (There was no air gap underneath the system), so that the shunt conductances (G) terms were modeled by taking a parallel combination of resistors which represent the resistance to current flow across the air gap and the resistance to current flow directly through the ground beneath the system.

Effect of Magnetite

Commercial ferrites are made by replacing the bivalent iron in Fe_3O_4 by manganese, zinc or some other element. The purpose for this is to reduce the conductivity, and, hence, the energy loss. The presence of a very small amount of bivalent iron can raise the conductivity to as high as 10^2 mho/m. However, Don Milligan of LANL found the conductivity of magnetite to be low unless he compacted it with a hammer. In the calculations, the conductivity of the magnetite was assumed to be small and calculations were performed with three relative permeabilities - unity, 83 and 500. The length of the ferrite plug was assumed to be 7 meters. Comparison with other ferrites makes it appear unlikely that the permeability would be much higher. If the electrical conductivity were high, the effect of the magnetite would be smaller as the current would flow on the outside of the plug and the skin depth would limit the inductance. The plugs would, in effect, look like an extension of the connector plates. In any event, the effect of the plugs is only dramatic at early times, where the highest permeability reduced the current on

the cable harness by factors of five to ten. At late times, the effect is about a factor of two.

Isolated Trailers

The isolation of the trailers after reference 1 was compiled is difficult to fit directly into the transmission line code. The reason for this is that there are two separate branches of uphole wiring with different characteristics. The first set is the support harness and the cables to trailers which were connected to the wellhead; these have a low impedance termination at late times and considerable currents flow on them. The second set is the cables connected to trailers which are isolated; these have a high (capacitive) impedance at late times and the currents on these cables will be low. The transmission line code uses an LU decomposition to solve the equations which are tridiagonal - the presence of the two branches cannot be solved by this scheme. Rather than go with a more complicated matrix solution, we chose to use a sequential method where the main code only includes the branch terminated in a low impedance. We store the rack connector plate voltage and the currents on the uphole wiring.

An auxiliary code was written which drives the cables to isolated trailers, using the rack connector plate voltage and the currents on the cable support harness. One feature is worth noting - the mutual inductive coupling from the support harness reduces the current on the instrumentation cables. A little thought about the sign shows that this is correct - the effect of mutual inductance is to generate an opposite current on a parallel wire.

SECTION IV
COMPUTATIONAL RESULTS
AND COMPARISON WITH MEASUREMENTS

Scoping Calculations

The results of the preliminary scoping calculations are shown in Table 1. The purpose of the scoping calculations were to set the basic physical conditions for the grounding and shielding plan, and to determine the effects of the conditions around the zero room and the air void space around most of the tunnel. The calculations assumed that the trailers were grounded to the wellhead, so only the total current on the harness and the cable plant was calculated. The leftmost column shows the conditions of the particular calculation - the driver was divided into early ($< 1\ \mu s$) and late (1-100 μs) contributions, and the early time driver was further subdivided into "hotspot" and "no hotspot" calculations, depending on whether or not a gamma rays were blocked from the entering the walls of the alcove containing the device. (In the actual construction, lead bricks were incorporated to produce an intermediate case.) The second column shows the soil conductivity, and the lowest reasonable value of 0.002 mho/m was included to produce worst case response. In the scoping calculations, the size of the void space between the metallic walls of the tunnel and the soil was varied between 10^{-4} meters (where it had no practical effect, the value was used because the technique could not accept zero), and 0.6 meters which was felt to be the largest reasonable value. The results shown in table 1 are currents, except for the last column which is the voltage appearing across the gap. The response is at early times was extremely sensitive to the assumed soil conductivity and the presence of the hotspot, and showed only minimal sensitivity to the presence of the void as the air conductivity became larger than the soil conductivity and shorted ;out the void. At late times, the results are less sensitive to the ground conductivity, but extremely sensitive to the presence of a void.

Table 1. Summary of preliminary results used for shielding/grounding study

	sigma	void	uphole #2	drift	main	uphole #1	gap V
no hotspot	0.015	10^{-4}	0.005	0.6	83	11	6
hotspot	0.015	10^{-4}	0.057	6.5	908	118	69
hotspot	0.015	0.6	0.242	27.9	1970	236	293
no hotspot	0.002	10^{-4}	1.550	24.5	359	64	378
hotspot	0.002	10^{-4}	17.00	269.	3950	698	4160
hotspot	0.002	0.6	21.60	327.	4330	776	5060
late time	0.015	10^{-4}	0.685	4.0	93	15	112
late time	0.015	0.6	93.50	290.	6680	2390	8150
late time	0.002	10^{-4}	1.590	4.0	74	37	804
late time	0.002	0.6	18.60	43.3	866	466	8840

Final Calculations

The set of final calculations is shown in tables 2 through 5, and in figures 4 through 14. In these calculations, the trailers have been assumed to be isolated and the effective size of the gap is assumed to be 0.15 meters. (The numerical code has been slightly modified during the preparation of this report to extend from early to late times in a single calculation, and the results are plotted on semilog plots. The change in time step produces a slight difference in the late time peaks.) Table 2 shows the quantities associated with uphole #1, and the effect of a variation of conductivity a factor of two above and below the nominal value of 10^{-2} mho/m. The second through fifth columns are the peak voltages with respect to distant ground of the zero room, the rack connector plate, the wellhead and the trailer. The last two columns are the total (common mode) currents expected on the support harness and the cable bundle. Table 3 summarizes similar quantities for uphole #2, and includes the voltage across the gap in the line of sight. Tables 3 and 4 show the effect of different assumed magnetic permeability for the magnetite, whose conductivity was assumed to be small.

Table 2. Soil conductivity study summary for uphole #1

sigma	zero room	rcp #1	wellhead #1	trailer #1	harness #1 (I)	cable bundle I
10^{-2}	33,700	33,700	662	11,200	314	9.3
5×10^{-3}	60,600	60,800	1140	18,200	259	16.3
2×10^{-2}	19,900	19,900	318	7320	315	5.7

Table 3. Soil conductivity study summary for uphole #2

sigma	gap	rcp #2	wellhead #2	trailer #2	harness #2 (I)	cable bundle I
10^{-2}	1270	52.9	22.5	52.9	10.7	.00036
5×10^{-3}	1710	67.7	38.2	67.7	8.7	.00225
2×10^{-2}	820	35.5	10.7	35.5	10.7	.00016

Table 4. Magnetite permeability study summary for uphole #1

μ_r	zero room	rcp #1	wellhead #1	trailer #1	harness #1 (I)	cable bundle I
83	33,700	33,700	662	11,200	314	9.3
1	33,700	33,700	662	10,700	315	8.2
500	33,700	33,700	662	14,000	311	15.6

Table 5. Magnetite permeability study summary for uphole #2

μ_r	gap	rcp #2	wellhead #2	trailer #2	harness #2 (I)	cable bundle I
83	1270	52.9	22.5	52.9	10.7	.00036
1	1260	52.4	22.5	52.4	10.7	.00036
500	1280	55.9	22.5	55.9	10.7	.00038

The time histories are shown in figures 4 through 14. The open circuit driver voltage is shown in figure 4 for the three conductivities, 0.01 (case 1), 0.005 (case2) and 0.02 (case3) mho/m. The driver consists of an early and a late time portion - the early time portion driven by prompt gammas and a late time portion between 1 and 100 μs driven by capture gammas. The early portion produces an open circuit voltage of 34 kV for the nominal case and the late time produces a open circuit voltage of about 4 kV. It should be noted that the impulse (time integral of the open circuit voltage) is much larger for the capture gammas, as the peak is smaller by about a factor of ten, but the duration is three orders of magnitude larger. The potential expected for the zero room is shown in figure 5. The potential at early times is the same as the open circuit driver, but the late time response is smaller by a factor of about two, indicating that about half of the late time Compton current returns by a more circuitous route. The late time zero room voltage is less affected by the ground conductivity than the early time voltage and is about 2 kV. The voltage at rack connector plate #1 is very close to the voltage at the zero room, as there is a lot of metal connecting the two. On the figures, there is no visible difference, and the tabular data shown a difference only in the last digit printed out by the computer for the low conductivity case. The wellhead voltage is shown in figure 7. The wellhead voltage signal is composed of two parts, a small signal induced by the currents on the uphole cable on the support harness and a larger diffused signal which peaks at 30 or 40 microseconds. Figure 8 shows the expected voltage at the trailer park compared with the voltage at the rack connector plate, only for the nominal ground conductivity. There is a pulse exceeding 10 kV driven on the uphole cables at early times, and after about a microsecond, the trailer park follows the rack connector plate, which has a 1 kV potential at 10 μs. The current on the harness and instrumentation cables are shown in figure 9. The current on the harness is larger as the resistance to ground of the harness support structure is about 1.2 ohms, while the isolated trailer has only a capacitance to ground. At late times, the potential of the wellhead and trailer park approach the rack connector plate at most of a kilovolt. Figure 10 shows the voltage calculated at the instrument alcove gap. The early time signal is very sensitive to the assumed ground conductivity, as the early time voltage is dropping rapidly. The late time driver is only slightly sensitive to the conductivity and, indeed the gap voltage is basically the same at late times as the zero room and RCP#1 - for times longer than the diffusion time scale, all of these voltages should be the same, as they are all tied together by metal. The expected voltage at rack connector plate #2 is shown in figure 11. The time history is similar to that of the gap voltage, but the magnitude is reduced. The wellhead #2 voltage is shown in figure 12, and is calculated to be about 1/3 of the RCP voltage. The trailers in park #2, in contrast, follow the RCP #2 voltage very closely. The harness and instrumentation cables common mode currents are shown in figure 14. The instrumentation cable common mode is predicted to be less than a milliamp, as a slow voltage is driving a capacitance. The harness current follows the wellhead voltage.

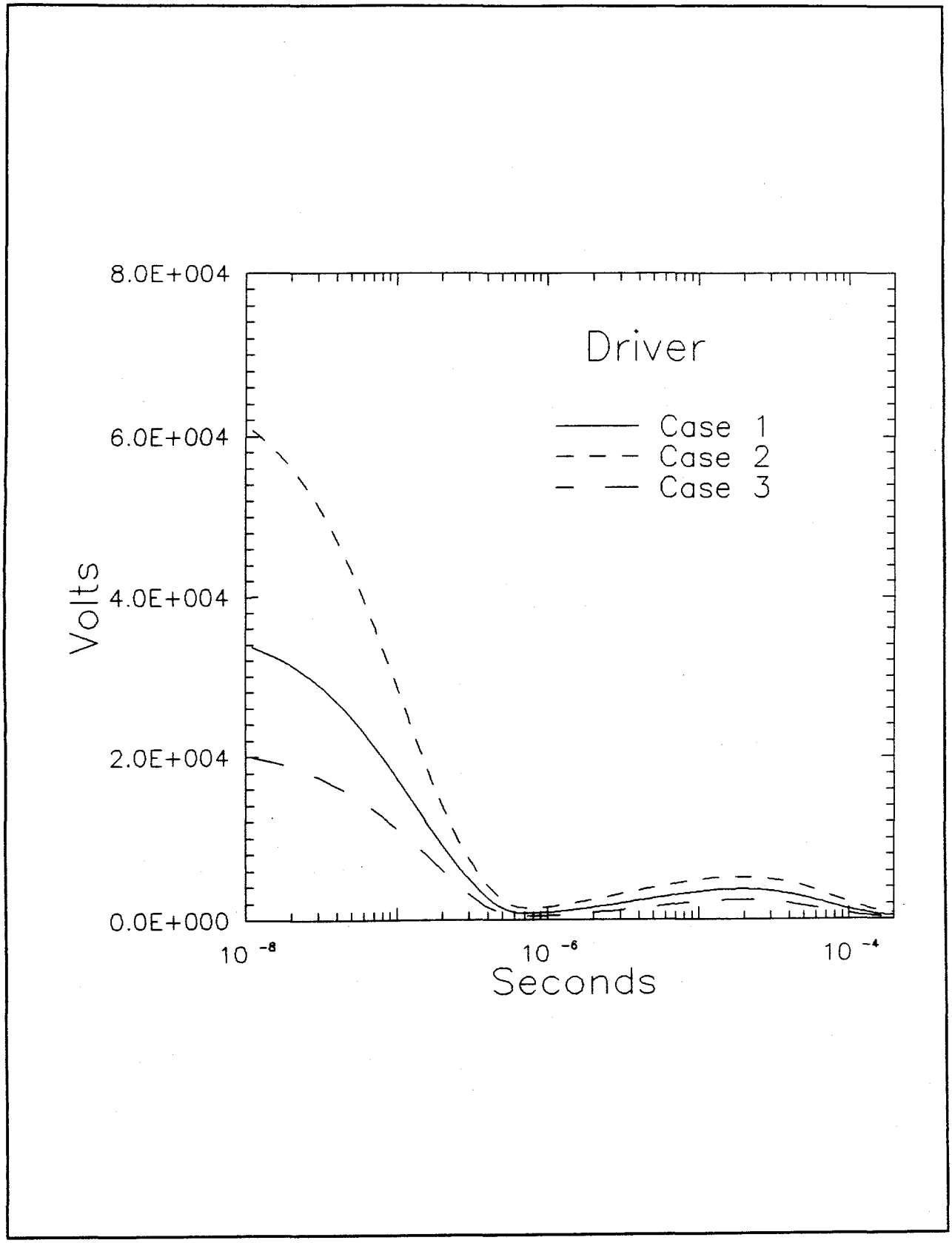

Figure 4 Open circuit driver voltage.

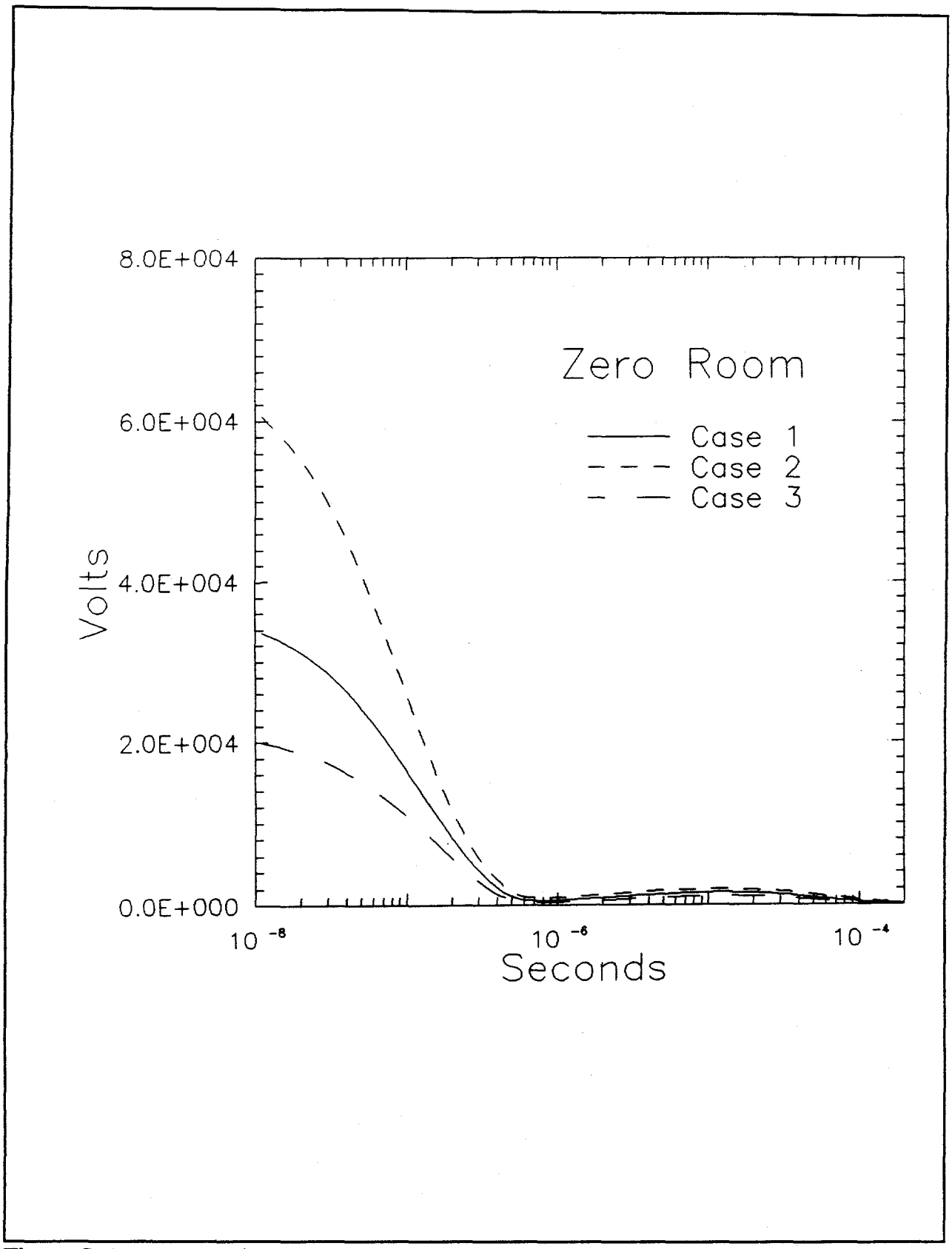

Figure 5 Zero room voltage.

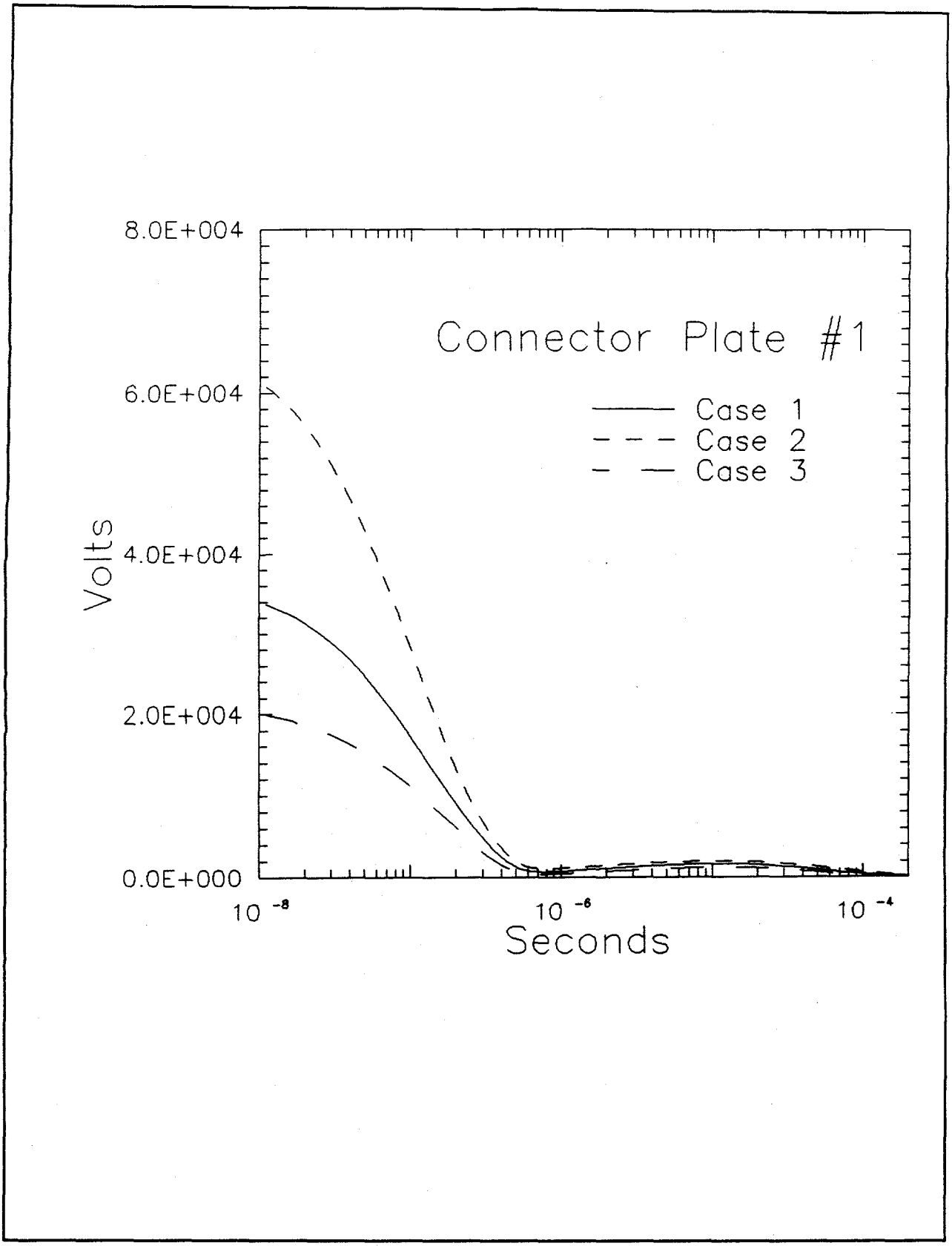

Figure 6 Rack connector plate #1 voltage.

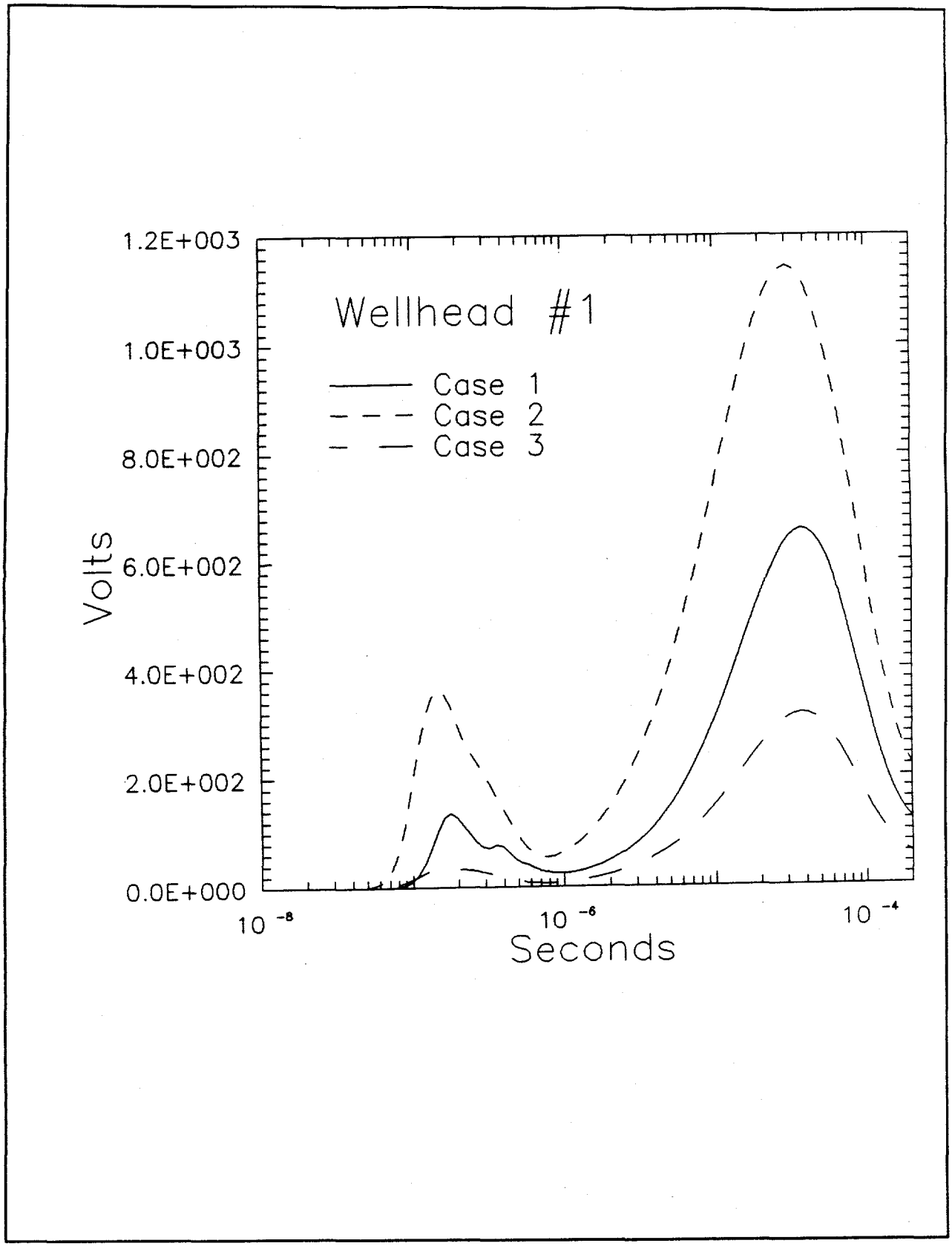

Figure 7 Wellhead #1 harness support voltage.

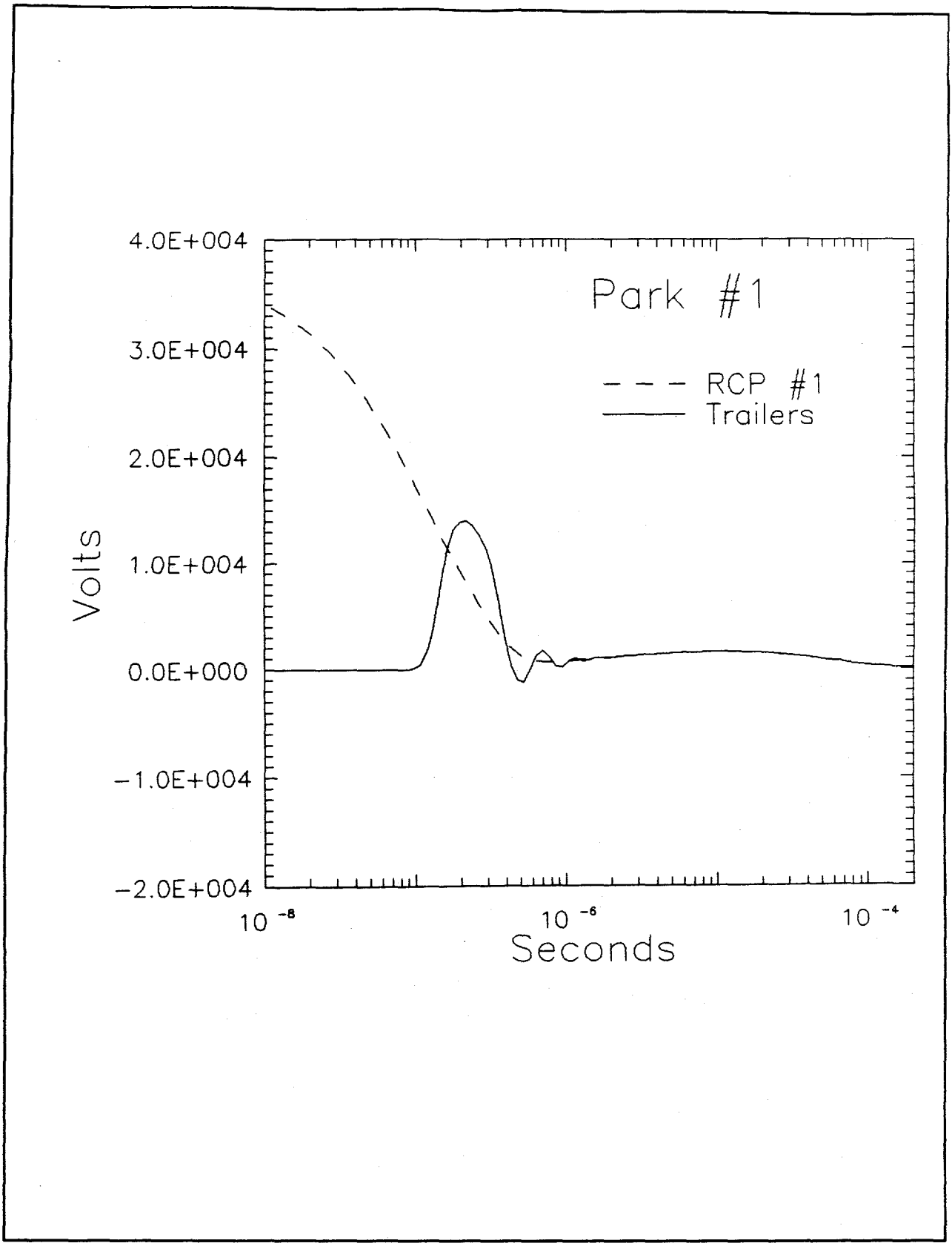

Figure 8 Wellhead #1 trailer and RCP voltage.

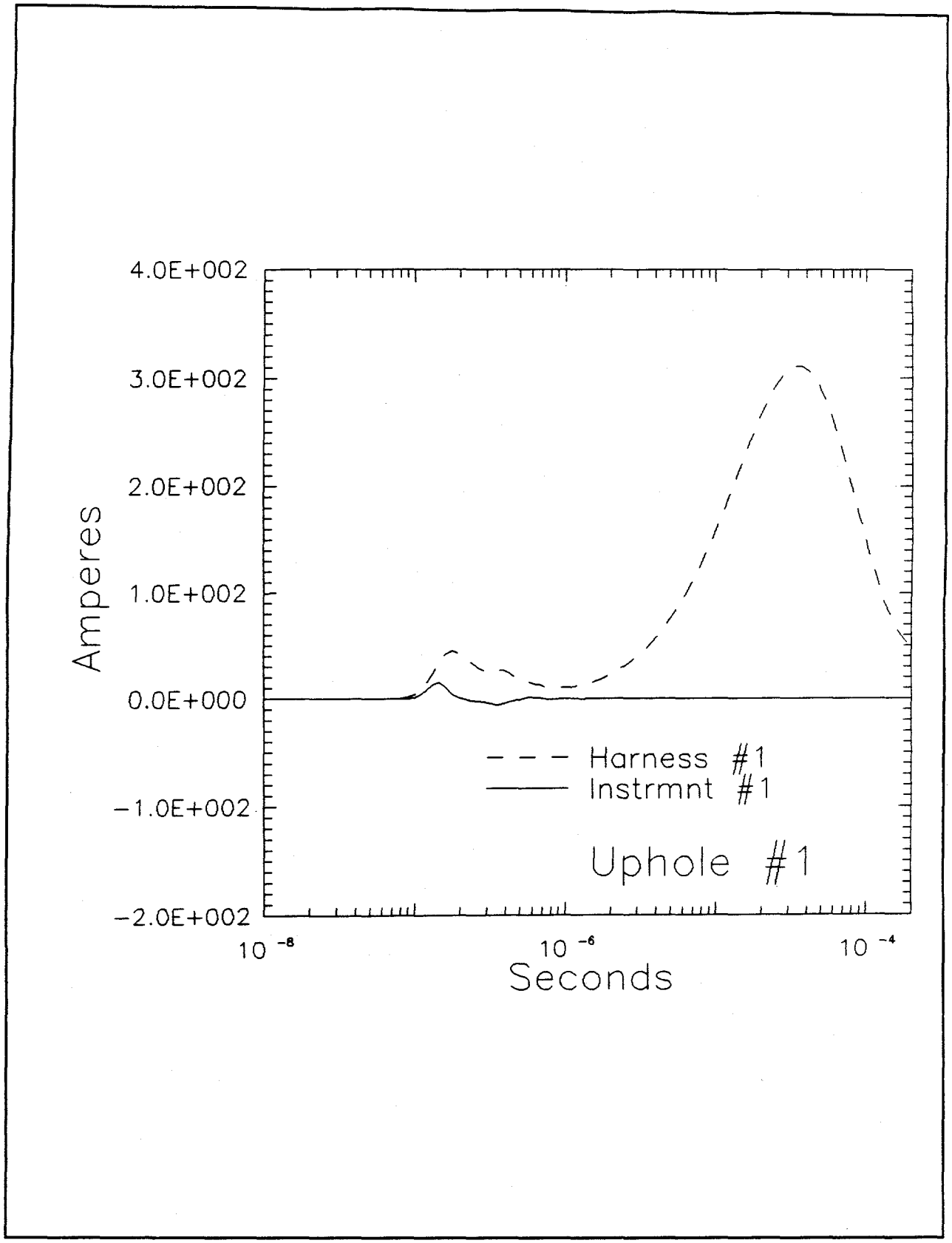

Figure 9 Wellhead #1 harness and instrumentation cable currents.

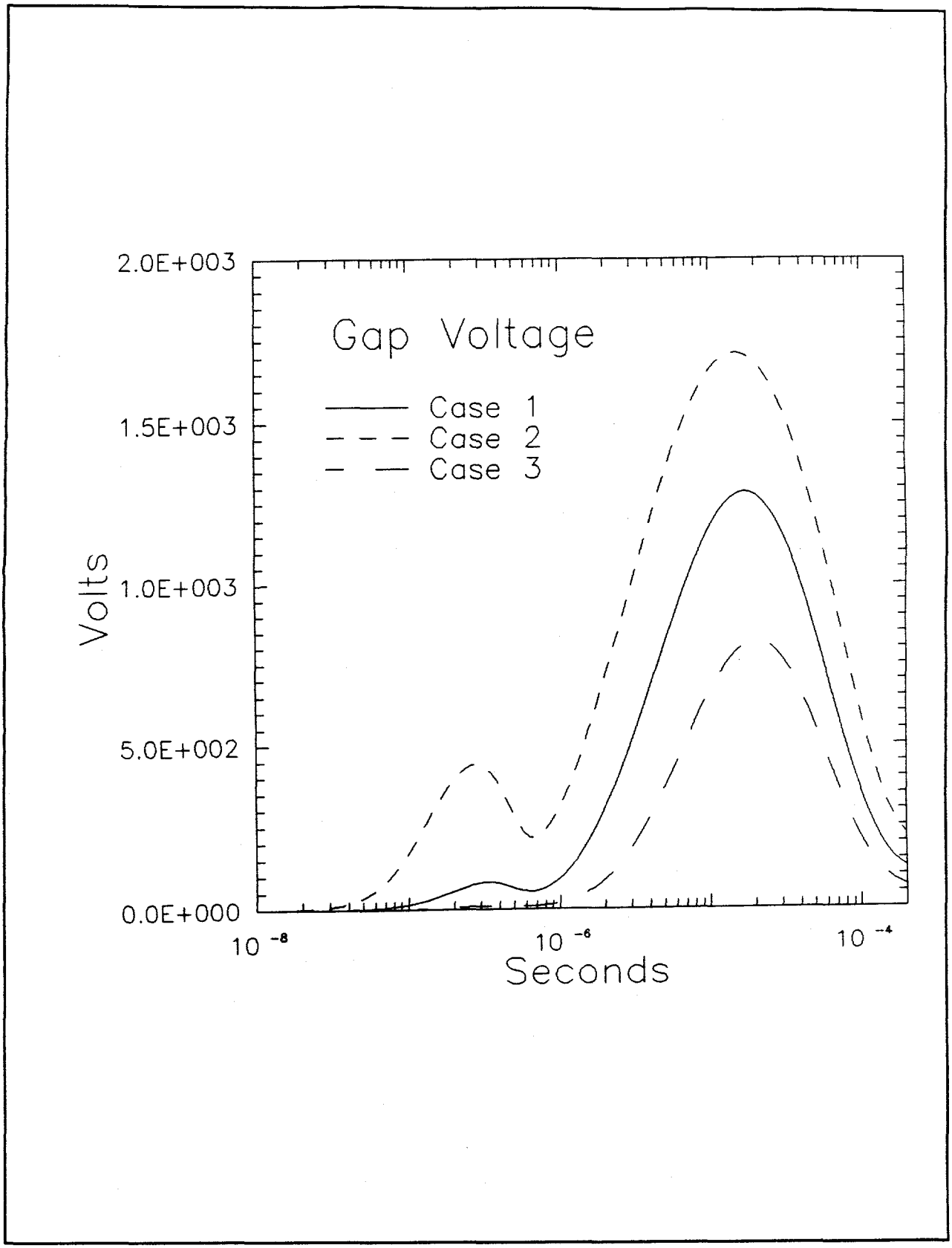

Figure 10 Instrument alcove LOS dielectric break voltage.

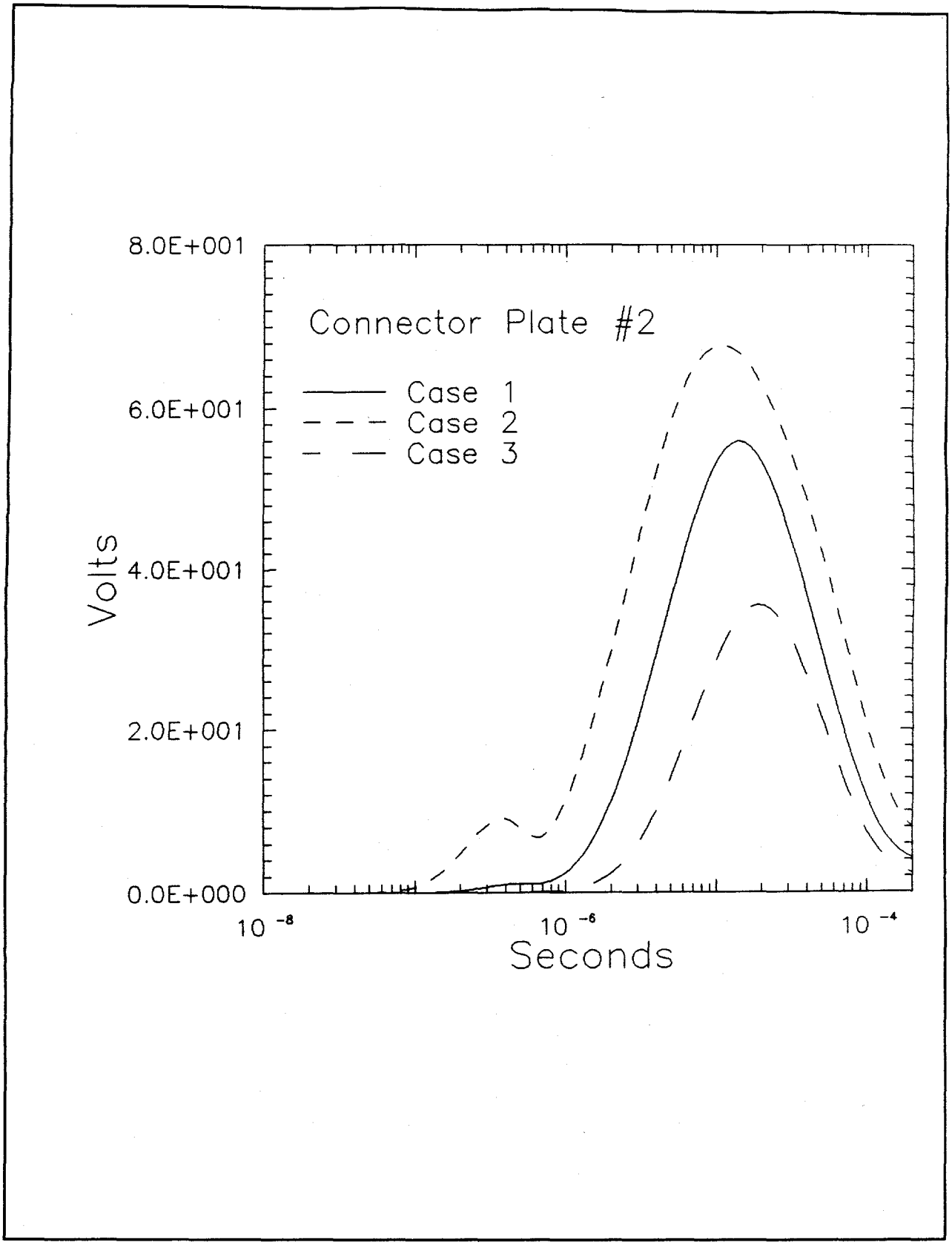

Figure 11 Rack connector plate #2 voltage.

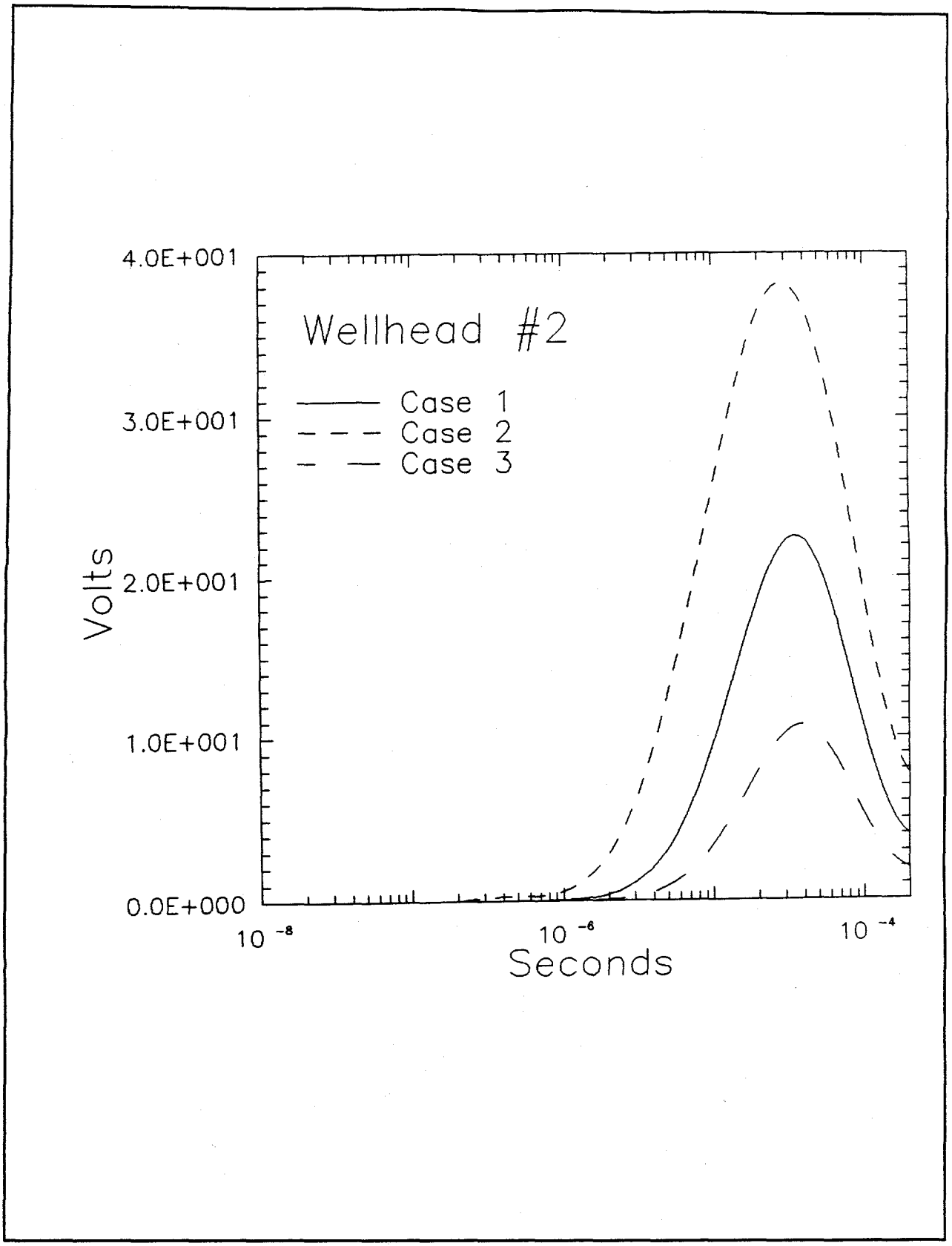

Figure 12 Wellhead #2 harness support voltage.

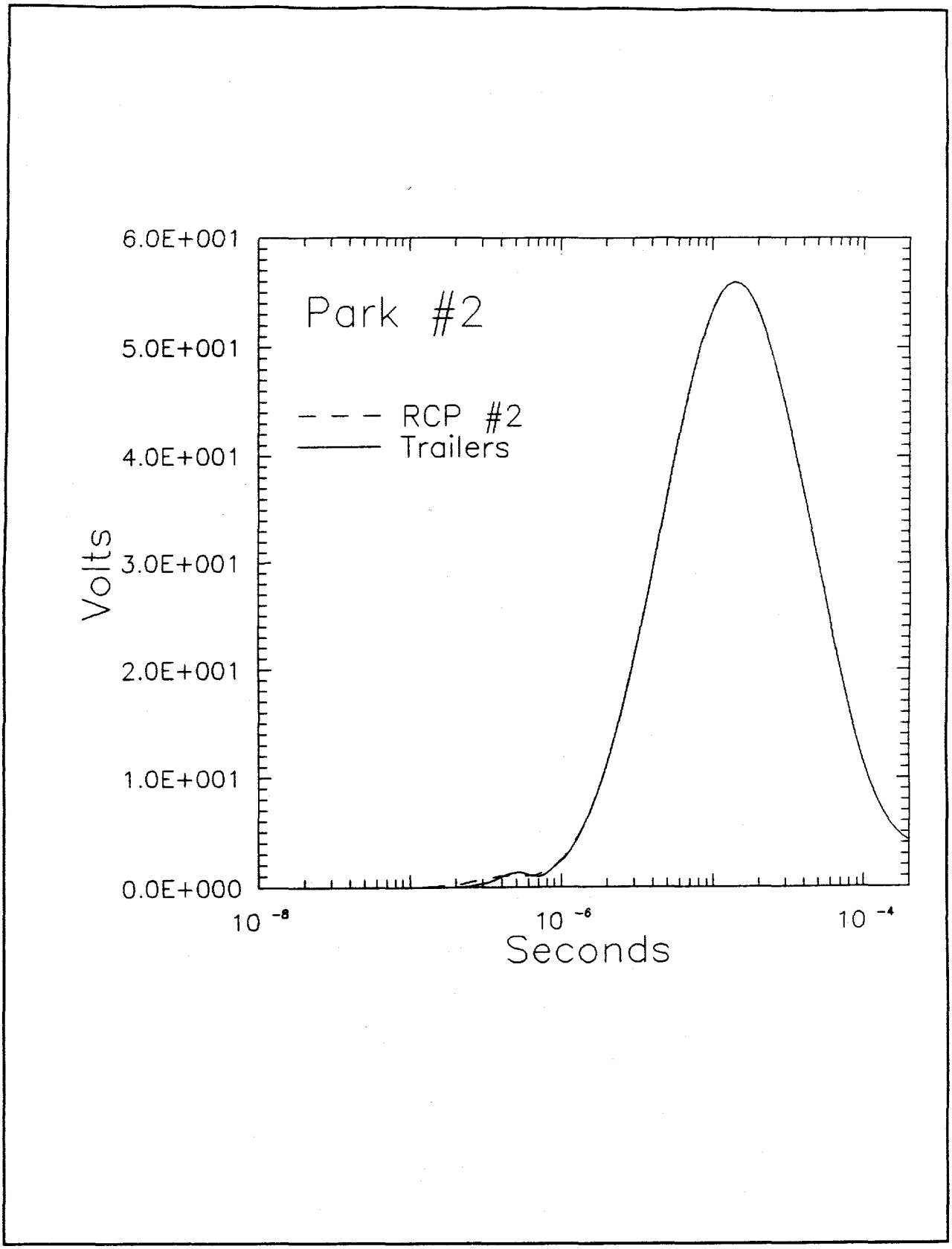

Figure 13 Wellhead #2 trailer and RCP voltage.

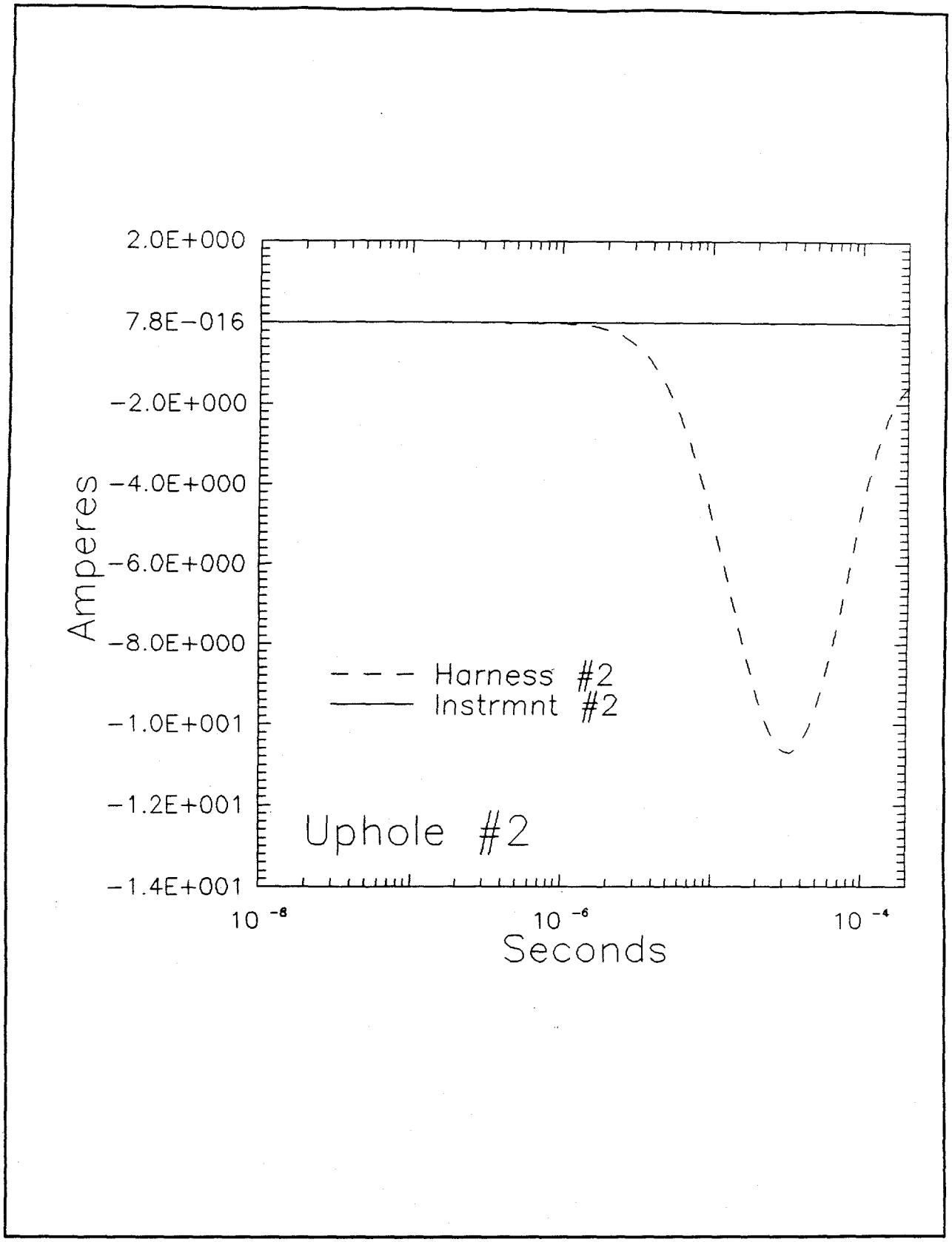

Figure 14 Wellhead #2 harness and instrumentation cable currents.

Data Comparison

In this section, we will look at the available data, proceeding from the measurements closest to the zero room outward, and comment on the comparison between the measurements and the observed data. The measurement closest to the zero room was a potential measurement on an earth probe near the RCP #1, TR224. The tip of the probe was placed in the soil at a distance between one and two meters from the RCP, and, in this location, would not measure the full potential between the RCP and distant ground. If the RCP were isolated, the potential would fall as 1/r and a couple of radii away would be sufficient for a full measurement of the potential. However, the walls of the zero room and much adjoining structure are also grounded and will come to the same potential as the rack connector plate; their scale length will determine how the potential falls off. Considering this and the support harness, it appears that the probe voltage with respect to the RCP will be a quarter or third of the full RCP potential. This would indicate a RCP voltage of 18-24 kV driven by the prompt gammas and 3-4 kV driven by the capture gammas. This compares with the expected 34 kV for the prompt and about 2 kV for the capture. The time scale of the capture signal is shorter than the pretest prediction for the voltage, and this time history is set by the combined neutron-gamma transport calculation. The voltage measurement between the RCP #1 and the corner of the zero room indicates that after a few microseconds, the zero room and the RCP come to the same potential, as expected in the calculations. Measurements after 90 μs are dominated by the apparent dump of a power supply for photodiodes.

At the top of hole #1, the situation is complicated by the apparent failure of some measurements. The pretest predictions expected the trailers to be driven to over 10 kV by the prompt signals on the uphole cables, and to rise to about 2 kV, following the RCP at about 10 μs. The wellhead, driven only by diffusion on the harness, would rise to a potential of about 600 volts at 30 μs. Three measurements were made, TR226 of the trailer to local ground, TR225 of the trailer to the wellhead and TR235 between the wellhead and local ground. As these three measurements of the voltage form a loop, the sum should be nearly zero at late times. However, TR225 showed about 13 volts at a few microseconds, then dropping to zero, TR235 showed similar early time signals, followed by a slow rise to 900 volts at 100 μs, and TR226 was similar to TR225. (Both TR225 and TR226 show odd behavior after the 90 μs power supply dump. We believe that both the wellhead and the trailer park must rise to the RCP voltage at some tens of microseconds, and are inclined to believe TR226 of the three, as 600 volts had been predicted, peaking at 35 μs. This is supported by the measurement of the current on the support harness of 25 amperes on one cable, so we would expect 50 amperes on both. This is smaller than the 300 amperes expected, and is not consistent with the 1.2 ohms measured earlier for the wellhead connection. The trace has a flat top, and we wonder if the current is not actually higher. Turning to current measurements on uphole #1, several tenths of an ampere were seen on cables (measurements TR230 and TR232) at the trailer bulkhead wall. It is tempting for the analyst to compare these with the bulk predicted common mode cable bundle current of 6-16 amperes, but these could as well be due to differential mode excitation, and, in the absence of large early time (<5 μs) voltages at the trailer, we believe that these currents are due to differential modes created when the common mode was bled off by ground losses on the uphole cable run. Two measured cables started with a current of about 30 amps at early times at the RCP (TR214 and TR228).

Turning to uphole #2, the cable runs are driven by the voltage of the RCP which is downstream of the breaks in the alcove LOSs. The voltage across the gap was expected to be 800-1700 volts, and the measurement (TR091) indicated less than 1 bit (40 volts). This is difficult to reconcile with the measurements of the voltages of the RCP #2 earth probe (TR092), the trailer- WH#2 (TR093) and the trailer-ground (TR094) in the tens of microseconds. The RCP earth probe measurement is far from clean, and this may be due to poor contact between the probe and the ground, but the other two traces are clean, have a rise time of about 50 μs, similar to that expected, and are a factor of several less than

the calculated voltages (the trailer to ground was expected to be 35-68 volts, and the wellhead to trailer voltage was expected to be 10-40 volts.) The observed voltages are 1/3 to 1/6 of those expected, and rest of the tunnel structure appears to represent a continuous conducting structure. We cannot find a plausible location where the remaining zero room voltage is dropped, and suspect a problem with the gap voltage measurement. The cable current at the trailer bulkhead wall (TR096, TR098, TR125) measurements for uphole #2 tend to have the same time history as the driving voltage. The sign convention on the cables is not clear, but with the trailer isolated, even a common mode current of 100 mA for 50 μs would require thousands of volts, as the capacitance of the all the trailers could only be a few nanofarads. The expected total common mode current in the calculations for the low conductivity calculation is only two milliamperes, so we believe that the late time currents seen are either differential mode, or that the trailers have been grounded. The similarity in shape would support either explanation.

Comments on Modeling

The bottom line on the analysis of the data is that the models employed greatly overpredicted the early time common mode signals on the cables on wellhead #1, but reasonably (within a factor of several) predicted the distribution of voltages and common mode currents in the tens of microseconds and later. We believe that the reason for the overpredicted early time signals is that the transmission line formalism used for the calculation of the cables connected to the isolated trailers did not have sufficient loss terms. The calculation for the cables assumed that for the whole length the cables were a bundle with an effective radius of 30 cm in a hole in the soil which had a radius of 70 cm. No account was taken of the conductivity of the magnetite or other backfill material (although the magnetic properties of the magnetite were taken into account). The conductivity of the backfill material was sufficient to slow down the common mode on the cabling, and figure 8 shows that the early time potential of the wellhead #1 trailer park is sensitive to the time for propagation/diffusion of common modes on the cables - if it were a factor of two or three slower, the late time drivers would dominate as is seen in the data. The modeling of early time response would have been substantially improved by the incorporation of the conductivity of the fill material.

The late time modeling seems to be consistent with the data for the voltages and support harness current. The late time driver appears to have been larger, but with a shorter time scale than expected from the transport calculations, and the factor of several agreement on the response between prediction and measurement is consistent with other underground test experience. The limiting factors are the knowledge of the effective gap size and the soil and concrete conductivity.

REFERENCES

1. Gilbert, J. L., "Preliminary Coupling Model," Mission Research Corporation, November 1988.

2. Gilbert, J. L., "Ledoux EMP Model," Mission Research Corporation, August 1989.

3. Sherwood, S., and V. van Lint, "Shielding/Grounding Model," Mission Research Corporation, November 1988.

4. Longmire, C. L., "Theory of EMP from Nuclear Surface Bursts," Los Alamos Nuclear Corporation, LANC-R-8, January, 1970.

5. Longmire, C. L., "On the Electromagnetic Pulse Produced by Nuclear Explosions," IEEE Trans on EMC, vol. EMC-20, p.3, February 1978.

6. Scott, J. H., "Electrical and Magnetic Properties of Rock and Soil," Air Force Weapons Laboratory, AFWL EMP 2-1, Note 18, May 1966.

7. Longmire, C. L.,and J. L. Gilbert, "Theory of EMP Coupling in the Source Region," Mission Research Corporation, MRC-R-546, January, 1980.

APPENDIX
GROUNDING AND SHIELDING PLAN

1. INTRODUCTION

This advisory report concerns the instrumentation to be employed at the U1A drift experiment to be performed by the Los Alamos National Laboratories. The particular focus of this report will be on the electrical noise injected into the instrumentation channels, especially those from sensors in the alcove marked D in the facility diagram, there the most sensitive measurements will be made. It is important that these noise levels be kept as low as possible; maximum interference levels, as seen in alcove D (they are boosted later), have been established at roughly 20 mV.

The principal parts of the problem include: determining the mechanisms by which soil current will be induced in the alcove area, and what the magnitude of this current will be; estimating how these currents will affect the equipment; and determining the interfering voltages which could result. The latter two of these will have to be considered for each of several stages of the signal path, including the run from the sensor area to the screen room,and that from the screen room to the surface. For each leg of the journey, different design options will be evaluated and compared regarding their effectiveness in shielding against interference.

2. ESTIMATED SIGNALS

Table 6. Worst case currents used for shielding/grounding plan

Alcove D	air gap		
soil conductivity	60 cm	15 cm	0 cm
.002	330 / 43	300 / 12	270 / 4
.015	30 / 290	14 / 70	7 / 4

Uphole cable #2	air gap		
soil conductivity	60 cm	15 cm	0 cm
.002	22 / 19	20 / 5	17 / 1.6
.015	.25 / 95	.12 / 25	.06 / 0.7

Uphole cable #1	air gap		
soil conductivity	60 cm	15 cm	0 cm
.002	780 / 460	740 / 120	700 / 40
.015	240 / 2400	1800 / 120	120 / 14

3. DESIGN OPTIONS

3.1 Alcove D

3.1.1 Baseline configuration

the baseline design for the alcove D equipment includes:

1. A dielectric break in each of two pipes connecting the sensors to the zero room.

2. A gap between the metal framing around the experiment alcoves and that around the zero room and Line-of-Sight path.

3. The pipes are grounded to the soil at several locations along their lengths.

4. There are two runs of solid-shield instrumentation cables between the sensors and corresponding screen rooms at the back of alcove D. The cable shields are connected to the metal pipe at the sensor end and to the screen room at the far end.

5. The screen rooms are grounded to earth (e.g. metal framing) at a point on the screen rooms close to their input and output cable penetrations.

6. The uphole cables have their shields connected to the screen rooms near the grounding point.

7. The uphole cable shields are connected to the well-head and to the instrumentation trailer shell at the surface.

This design depends of the performance of the cables' solid copper shields. The copper shielding on standard 0.141" cujac is 16 mils; the diffusion time through this thickness is 6 microseconds. The maximum time constant of interest is taken to be 100 μs for the slow pulse and 2 μs for the fast pulse.

Since the diffusion time is much less than the slow time, the slow currents will generate a noise voltage equal to the current multiplied by the shield resistance over the entire length. The DC resistance of the shield is 6 mohm/m, yielding a total nose signal from the sun of 6 mohm x 20 m - 120 mV/amp, plus a small contribution from the connectors. We assume that, at the worst, 10% of all the current in the system might flow on one cable; even though there may be more than 10 cables, or other paths for the current to flow, one cannot be assured of a predictable, even current distribution. For an alcove current of 300 slow amps, or 30 amps per cable, the resulting noise magnitude would be 4 V, which is clearly unacceptable by the criterion given earlier for signal magnitudes.

The fast time is about 1/3 of the diffusion time, so the noise voltage will only be about $e^{-3}=.05$ times as big.

Thus the noise voltages during the fast pulse, with magnitude 33 amps per cable, will be 200 mV.

Even if all but 1 m of the cable run were enclosed in a thick (i.e.many skin depths thick at 100 μs) conduit, the interference produced in 1 m of copper shielded cable with two connectors by the slow pulse would still be 10 mohm x 30 A = 300 mV.

Three alternatives have been considered to alleviate this problem. These are addressed below.

3.1.2 Option 1

1. Eliminate the air gap in the zero room, thereby reducing the worst-case currents 270A early and 4 A late.

2. Enclose all but 1 m of sensor cable in a conduit (e.g. 1/8 in steel to provide skin-depth isolation even at 100 μs). Use solid shield cable and screw-type connectors (e.g. Cujac and SMA connectors) for the 1m section. Braid shielded cable would be acceptable inside the conduit.

Steel has the advantage of a high magnetic permeability (about 200 times that of most substances for cold rolled steel). Thus, the diffusion time is much longer; in 100 μs, current sill diffuse into steel only 11 mils. The attenuation due to a thick steel pipe will be exp(-t/11 mils); thus a 1/8 inch thick pipe will cut the noise by many orders of magnitude (essentially to zero). The steel pipe must be solidly grounded to the structure at each end, through the screen room or supports, and terminated in a steel junction box from which the cujac leads will issue. The ends of the conduit must make solid contact with the junction box and the screen room around the entire circumference.

The impedance of a well-tightened SMA connector is about 2 mohms, so the transfer impedance resulting from the Cujac lead will be (assuming two connectors per lead) 4 mohm + 6 mohm per meter of lead length; thus a 1 meter lead will produce 8% of the noise produced by an entire run of cujac.

The interference produced by the early time worst cast current of 1/10 of 270 A would be 10 mohm x .03 (for skin effect) x 27 A, or approximately 8 mV. The interference produced by the late current pulse would be 10 mohm x 0.4 A, or 4 mV.

While the improvement from reducing the air gap to zero is clear, the practicality is questionable. As Table 1 illustrates, reducing the air gap in the exposed region from an average of 60 cm to an average of 15 cm reduces the slow interference pulse by a factor of 4, as compared to a factor of 75 for a zero gap. This produces an estimated interference of 70 mV for the slow pulse, which is inconsistent with the interference requirements.

3.1.3 Option 2

1. Isolate the pipe section containing the sensors from the grounded support struts using dielectric pads.

2. Enclose all but 2 m of sensor cable in a conduit, and use solid-shielded cables and screw-type connections for the 2m sections.

For a set of four pads at each of ten locations, with pads measuring 6" x 2" x .5", the total capacitance across the pads, (i.e. between signal shield and surrounding earth) would be 750 pF. The source voltage driving currents along the path for this case has been calculated at 10 volts per amp in the table above, or 3200 volts for the worst case; for a time constant of .5 μs, the current will only be 4.5 amps. In this case, the current across the dielectric break should also be included. The capacitance of this break is 100 pF; the dV/dt across it is estimated to be 10 kV/μs, which adds a current of 1 amp to total 5.5 amps. The slow current would be 1/50 of this, or .1 amp. Thus, the fast current is reduced to 3% of its previous value, and the slow current is reduced to .06%. The interference levels with this option would

then be < 1 mV for both the fast and slow components.

While it's not possible to demonstrate by these calculations that braid-shielded cables and screw-type connectors are unacceptable for the short runs outside the conduit, it is recommended that solid-shield cables and screw-type connectors be used exclusively outside the conduit. Unestimated high-frequency noise components could be generated by the source and zero-room, which would couple preferentially through braid shields.

3.1.4 Option 3

1. Isolate the sensor pipe from ground by dielectric pads, as in Option 2.

2. Use solid copper shielded cables from the sensors to the screen room, without an overall conduit.

In this case the fast signal is reduced to 2 mV and the slow signal is 1.2 mV.

3.2 Uphole cable #2

3.2.1 Baseline configuration

The standard design for this portion of the run is merely to run the cable bundle by itself through the uphole, with the shields of all the cables grounded to the local ground at each end. The length of the run is 400m. There will be approximately 200 cables run through the uphole, roughly 1/3 of these RG22 twinaxial cables which will carry the sensitive measurements.

RG22 has the same shield resistance and thickness as cujac - the interference fields will diffuse through the shield and produce an IR voltage drop between the ends. We will again assume a worst case of 10% of the current on any one cable, even though there are many more than 10 cables. Times on the order of tens of microseconds or longer may be required for the current to work its way onto the cables which are not on the outside of the bundle, and therefore it amy only be those cables on the outside which carry a large fraction of the total current at earlier times. The voltage generated along the cable shield will be 95 / 10 x (6 mohm/m x 400m)=24 volts for the slow pulse and 0.3 x 33/10 x (6x400)=.2 volts for the fast pulse. The slow pulse is clearly the trouble spot.

RG22 is a dual conductor cable, so the signal itself is just the difference between the two inner conductors. Thus, the 24 volts calculated above will appear across both of these conductors relative to the common shield; the best readily attainable common mode rejection for this type of cable is about 30:1, which would result in a signal-channel interference voltage of 24/30=0.8 volts. Even this unacceptable result will require great care as to the termination impedances of the inner conductors and common-mode rejection of the receiver amplifier. In particular, the two inner conductors must both be terminated in identical impedances; even a small impedance mismatch will induce differential mode excitation in the cable, sacrificing much of the benefit of the twinaxial cable.

The common mode signal that would appear on the inner conductors is equal to the termination resistance (which should be 47 ohms for RG22) divided by 47+12 ohms (the resistance of 400 m of inner conductor)=0.8 times the voltage drop across the ends of the line, or 20 volts. Thus, the differential amplifier would have to have a CMRR of 40 db in order to bring the noise from this common mode, neglecting the noise calculated above, to 10 mV alcove equivalent.

3.2.2 Option I

This is the same as option 1 for the sensor cables: eliminate the gap around the zero-room conducting liner. In effect, this decreases the late time driver by a factor of 60, which results in an estimated interference level of 13 mV for the RG22 cables. Care will be required to assure the 30:1 common mode rejection. If the down-hole amplifier gain is at least 10x, then the equivalent noise level at the sensor is 2 mV.

As is the case of the sensor cabling, if the air gap is reduced to only an average of 15 cm, the improvement is only a factor of four. In this case, the residual interference is 200 mV, which is marginal.

3.2.3 Option II

Provide another conductive path between the ends of the uphole cables i.e. run a number of large gauge copper wires along with the RG22's and ground them at both ends; the purpose of this would be to divert some of the uphole current away from the cable shields.

The basic idea is to reduce the voltage difference between the surface and the alcove as much as possible. This could take the form of an extra series of shunt cables, kept on the outside of the cable bundle so as to absorb maximum current; in this case, the resistances of these would be added in parallel to that of 10 RG22's (shield resistance of 10 through 400m; 0.24 ohms). A pair of #1 copper cables, for instance, straddling the bundle, would put 0.7 ohms in parallel with this, thereby cutting the voltage to 20%. This approach is somewhat uncertain in that the noise generated on cables far from the shunts might not be attenuated by as much as the average.

A superior (but probably impractical) implementation of this idea would be to have the cables enclosed in a conducting pipe or mesh.

3.2.4 Option III

Float the recording trailer at the surface (i.e. do not connect the cable shields to earth ground at the uphole recording site). This has the potential of greatly attenuating the current that would flow on the cables. This is a familiar practice at the Nevada Test Site. It requires using a dielectric-shaft motor generator set for instrumentation power, mounting the trailer on dielectric supports (e.g. foam blocks), using relays or isolation transformers in the timing signal lines, and using a knife switch to ground the trailer shell for personnel safety during pretest checkout. It is also important to provide for disconnecting any other conductors, such as intercom and telephone wires, prior to the test.

The time for a signal to reach the surface is 1 μs; even the fast pulse will, for the most part, be slowly varying over this time. Therefore, the only currents which will flow on the shield if it is ungrounded at one end are those which will capacitively couple from the ground to the shield. This capacitance is 10 nF, and the estimated soil resistance 2 ohms, so the maximum current expected for the slow pulse would be 95 amps x 2 ohms / 50 μs x 10 nF=0.4 amps; the voltage drop, 0.1 volts; the noise .3 mV. The additional capacitance to earth ground of the instrumentation trailer would be small compared to the capacitance of the uphole cable run.

3.3 Uphole Cable #1

Interference in Uphole Cable #1 is similar in mechanism to Cable #2, with the following differences:

1. The driving currents are larger by approximately a factor of 30.

2. Most of the signals are carried on coax cables, rather than twinax.

Using the same baseline as for Cable #2, the common-mode signals (center conductor vs. shield) could be as large as 750 volts. Even though most of the signals are expected to be large, interference at this level is not acceptable.

The solutions to this problem are the same as for Cable #2:

1. The driver can be reduced by more than a factor of 100 by reducing the air gap to zero. However, the reduction for an air gap of 15cm compared to 60 cm is only a factor of four.

2. Isolating the cable shields and recording trailer from ground at the uphole recording site will effectively reduce the interference by a large factor.

It is important to note that with the floating trailer concept, separate recording trailers must be used for the two cables. Providing a path by which current can flow up through one cable bundle and down another could have disastrous consequences.

4. SUMMARY OF INTERFERENCE ESTIMATES

Table 2 presents a summary of these estimates. It is clear that the baseline configurations, which were formulated prior to appreciating the effect of a gap between the tunnel-lining conductors and the earth, will not meet the test interference requirements.

On balance, either Option 1, 2 or 3 is acceptable for the cables between sensors and screen room. Option 1 (small air gap) by itself requires that the gap be truly small. Implementing a combination of Option 1 and either Option 2 or 3 (smaller air gap in zero room and dielectric pads at the sensor pipe section) would provide a margin of safety, with reasonable tolerance in the air-gap.

Table 7. Estimated noise voltages

Alcove D fast/slow pulse - interference in mV	air gap		
	60 cm	15 cm	0 cm
baseline	120 / 4000		
option 1 small gap, conduit		8 / 70	8 / 4
option 2 diel pads, conduit	< 1 / < 1		
option 3 dielectric pads	2 / 1.2		

Assuming: worst case conductivity
dielectric pads are installed (option 1)
maximum of 10% of current flows on one cable

Uphole #2 interference in coax / twinax in mV	air gap		
	60 cm	15 cm	0 cm
baseline	24000 / 800		
option 1 small air gap		6000 / 200	400 / 13
option 2 current shunt	4800 / 160		
option 3 float trailer	10 / < 1		

Assuming: worst case soil conductivity
30:1 common mode rejection for RG22
maximum of 10% of current flows on one cable

For the Uphole Cable #2 interference, Option 1 (smaller gap in zero room) will result in acceptable late time interference. Option 2 (current shunting) is probably impractical for typical downhole cable installations. Option 3 (floated trailer) is an excellent solution, which is particularly well suited to interference on a relatively slow time scale.

For Uphole Cable #1, very large interference is possible in coax cables unless some measure of protection is provided. Fortunately, the same measures needed for Cable #2 would provide reasonable protection for Cable #1.

5. RECOMMENDATIONS

Recommendations will be made at two levels: less and more conservative.

5.1 Less Conservative

In additional to the baseline configuration, the following are recommended:

1. Mount the sensor pipe sections (i.e. downstream from the dielectric breaks on dielectric pads, so that they are connected to ground only through the cable conduits and screen room ground point.

2. Enclose most of the sensor cable run in a steel conduit or run solid-shield cables from sensors to screen room. Connect the sensor cable shields to the conduit at entry and exit points. Use braid shielded cables inside the conduit, if desired.

3. Isolate the uphole cable bundles and the recording trailer shells from uphole earth. Use separate recording trailers for separate uphole cable bundles.

5.2 More Conservative

In addition to the measures recommended above, decrease the air gap between metallic liner and earth around the zero room as much as possible.

5.3 Checkout Recommendations

A test setup is recommended for assuring that the uphole cables are sufficiently noise-proof. Such a setup would include a separate grounding block for the lower end of the uphole cable shields,which can be temporarily electrically isolated from the local ground for test purposes. A test generator would send a current pulse which mimics that expected from the explosion into the grounding block, and up through the cable shields; the current would return through the soil. The signal leads would be connected together and to the shields at the down-hole location. The shields would be connected together to the well-head at the uphole end. In this configuration, the spurious signal at the surface resulting from the applied current pulse could be measured directly on each cable to determine its shielding effectiveness. For slowly varying currents which are expected to cause the trouble, the current applied at one end will be equivalent to that generated along the length by the source itself.